NANO LETTERS

pubs.acs.org/NanoLett Letter

Rapid, in Situ Neutralization of Nitrogen- and Silicon-Vacancy Centers in Diamond Using Above-Band Gap Optical Excitation

Christian Pederson,*,# Nicholas S. Yama,*,# Lane Beale, Matthew Markham, Mark E. Turiansky, and Kai-Mei C. Fu

Cite This: *Nano Lett.* 2025, 25, 673−680 Read Online

ACCESS | Metrics & More | Article Recommendations | Supporting Information

ABSTRACT: The charge state of a quantum point defect in a solid-state host strongly determines its optical and spin characteristics. Consequently, techniques for controlling the charge state are required to realize technologies for quantum networking and sensing. In this work, we demonstrate the use of deep-ultraviolet (DUV) radiation to dynamically neutralize nitrogen- (NV) and silicon-vacancy (SiV) centers. We first examine the neutralization of NV by correlating the NV^- and NV^0 spectra, indicating > 99% polarization into NV^0. We then examine the time dynamics of SiV^- photoluminescence, observing an 80% reduction of intensity within a single 100 μs DUV pulse. Finally, we demonstrate that this DUV-induced bleaching is accompanied by a dramatic increase in the SiV^0 population that is robust to extended periods of near-infrared excitation. Our results indicate the potential of above-band gap excitation as a universal means of generating neutral charge states of quantum point defects on demand.

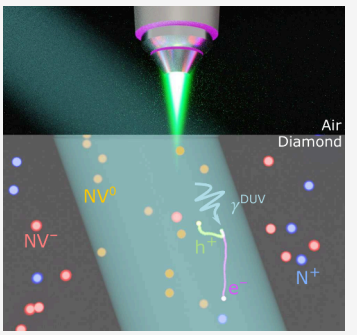

KEYWORDS: *neutral silicon vacancy, diamond, above-band gap excitation, neutralization*

Optically active, quantum point defects in solid-state host crystals have shown promise as a platform to implement a wide range of quantum technologies.[1−4] Generally, it is ideal for the defect to remain in a particular charge state; e.g., the negatively charged nitrogen vacancy NV^- for quantum sensing[5] or the negatively charged silicon vacancy SiV^- for quantum networking,[6] with neutral SiV^0 also showing promise.[7] Different charge states of the same defect have vastly different optical and spin properties which prevent the defect's use when in the incorrect state.

Control of defect charge states can be achieved through a range of techniques involving chemical, electrical, and optical processes. Chemical techniques, such as passive Fermi-level engineering via bulk doping of the host lattice[7−10] or functionalization of the surface for near-surface defects[11−16] are limited by the challenge of obtaining both n-type and p-type doping in a single wide band gap material[17] and rely on equilibrium conditions which may not be reached on practical time scales. Active electrical Fermi-level engineering[18,19] similarly relies on equilibrium conditions. Even in cases in which Fermi-level engineering can be achieved, unintended ionization of the defect is often unavoidable, so an active method of modifying the defect charge state *in situ* is still necessary. Alternatively, the long-lived nature of nonequilibrium states opens up methods for charge state control. Nonequilibrium control can be achieved by optical, electrical,[20] or combined optical/electrical[21] carrier generation. Intragap optical excitation has been used to demonstrate long-lived optical storage with the NV center,[22,23] neutralization of NV centers,[24,25] and stabilized SiV^- emission after prolonged exposure to blue light.[26] Furthermore, optical ionization requires no alteration of the sample, can be extremely rapid, and can even be tuned to selectively ionize a specific defect.

Recently, selective intragap optical excitation has been used to ionize an ancillary defect to control the target defect charge state via photogenerated carriers.[27−30] This technique, known as "photodoping", has revealed a large disparity between charged and neutral defect carrier capture cross sections due to Coloumbic attraction. Negative NV^- centers possess extremely large hole capture cross sections while neutral NV^0 show negligible charge capture.[27] These results suggest an interesting alternative charge state control method: the generation of free charge carriers by above-band gap excitation, which then preferentially neutralizes charged defects.

Utilizing above-band gap excitation poses unique experimental challenges in diamond; diamond is an indirect semiconductor with a large band gap of 5.5 eV corresponding to a deep-ultraviolet (DUV) wavelength of 225 nm. Not only are excitation sources at these wavelengths limited, but microscope optics optimized for visible or infrared (IR) are often absorptive at DUV. Furthermore, the dynamics of photoinjected carriers in diamond are complex, as tightly

Received: September 20, 2024
Revised: December 17, 2024
Accepted: December 18, 2024
Published: December 31, 2024

https://doi.org/10.1021/acs.nanolett.4c04657
Nano Lett. 2025, 25, 673−680

bound excitons form, diffuse, disassociate, and reform, generating free charge carriers which may be captured by defects.[31] Nevertheless, a body of existing work has demonstrated the effectiveness of DUV excitation at neutralizing defects in diamond by minutes-to-hours of exposure to UV before measurement. Neutralization of nitrogen and nitrogen-vacancy-hydrogen (NVH) complexes was observed after exposure to a Xe arc lamp[32] and 215 nm laser.[33] DUV exposure was integral in assigning the 1.31 eV emission to the neutral SiV center.[34] These results suggest that DUV excitation is defect agnostic, unlike intraband-gap excitation, and thus a powerful tool for charge control. Still, many questions remain regarding the time-scale of ionization, power requirements, achievable charge state polarization, and operation temperatures, all of which are critical in establishing DUV excitation as a practical technique for quantum technologies.

In this work, we demonstrate the integration of DUV excitation into a cryogenic visible/IR confocal microscope. We use this setup to demonstrate the effectiveness of DUV excitation in neutralizing the two most studied defects in diamond, NV and SiV, whose neutral and negative charge states can be detected through photoluminescence (PL). Time-resolved measurements reveal that the neutralization occurs on time scales competitive with conventional intragap photodoping, without the need for an ancillary defect. Furthermore, we observe an up to 80% reduction in SiV^- PL within a single 100 μs DUV pulse at power densities much lower than what is needed for direct ionization by intragap excitation. We then utilize DUV as a means of studying the spectra of SiV^0, a defect which exhibits long spin coherence times and stable, spin-dependent optical emission[7,35] but has been historically difficult to observe due to its unusual temperature dependence and tendency to bleach.

The experimental setup is illustrated in Figure 1a. A DUV HeAg pulsed laser (Photon Systems) emitting approximately 3 μJ of 224.8 nm light per 100 μs pulse is focused onto the diamond sample at an oblique angle between the PL collection objective and sample surface to circumvent the high UV absorption coefficient of the microscope optics. When focused onto the diamond, the DUV forms an approximately (1 mm × 2 mm) elliptical spot. Off-resonant continuous-wave (CW) excitation (532 nm for $NV^{0/-}$ and SiV^-; 830 nm for SiV^0; spot sizes of approximately 0.7 and 1 μm, respectively) and collection of PL are performed perpendicular to the sample surface through a visible-to-near-infrared (NIR) confocal microscope (SI.1). The DUV laser operates at discrete pulse rates tunable from 1−5 Hz.

Two different single-crystal diamond samples grown via chemical vapor deposition (CVD) are studied. The PL spectra in sample A (SC Plate CVD, Element Six, [N] < 1 ppm, [B] < 0.05 ppm) was doped during growth with nitrogen and annealed to 1200 °C for 2 h under high vacuum (10^{-7} mbar) and is dominated by NV center PL with no observable signal from SiV. Sample B was doped during growth with 0.1−0.3 ppm of silicon; no treatment was performed after growth. It is spectra is dominated by SiV with no observable NV signal.

DUV photons incident on the diamond generate charge carriers by excitation of valence electrons into the conduction band. During the subsequent, complex charge kinetics, some of the generated excitons and free charge carriers are trapped by impurities.[31,36] Capture of charge carriers at deep impurities has been observed to significantly reduce the lifetime and diffusion length in doped diamond compared to higher purity samples.[31] Due to the Coloumb interaction, electrons and holes are attracted to and are captured preferentially at oppositely charged defects, respectively, generating neutral defects. The neutralization of charged defects by optical carrier generation has been experimentally reported in smaller band gap materials (e.g., silicon) at low temperature, specifically to neutralize shallow donor qubits[37] in p-type material. While direct ionization by incident DUV photons is possible, the low power density of the DUV laser at the diamond sample, coupled with *ab initio* calculations of the ionization cross sections, suggests that direct ionization events are comparatively rare (SI.2).

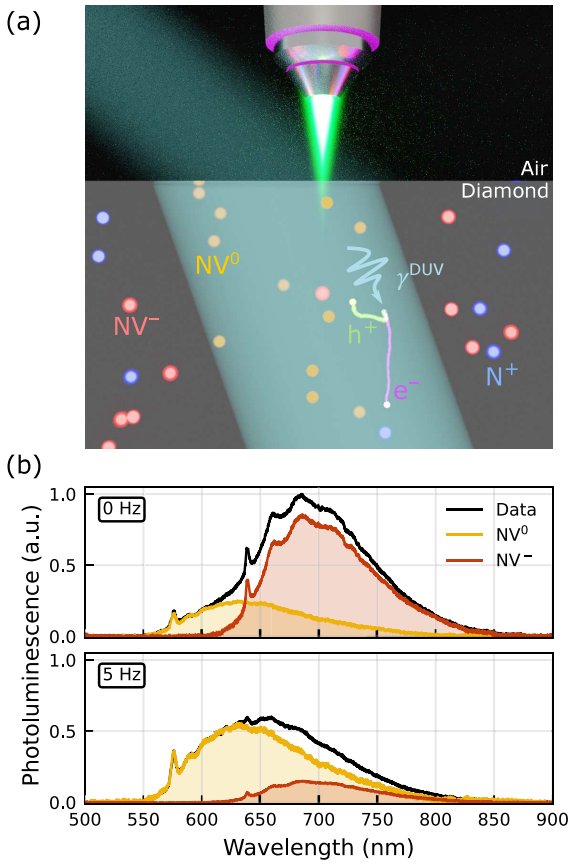

Figure 1. Neutralization by DUV. (a) An illustration of the experimental setup. The DUV laser illuminates the sample from an oblique angle while a confocal microscope simultaneously performs a PL measurement. The DUV photon generates an electron and a hole in the diamond host lattice which are preferentially captured by charged defects (here NV centers and substitutional nitrogen) as assisted by the Coulombic interaction. (b) In Sample A, when the DUV laser is off (top) the signal is dominated by NV^-. When the DUV laser is on (bottom), the PL spectrum is dominated by NV^0. Spectra were taken under 8 μW of 532 nm probe excitation at room temperature. Details of the spectral decomposition are discussed in SI.3.

Figure 1b shows PL spectra of NV centers in Sample A, decomposed into the neutral NV^0 and negative NV^- contributions under DUV excitation. Without the DUV (top panel), the signal is dominated by NV^- with a small amount of NV^0 due to charge cycling induced by the 532 nm probe.[38] With the DUV on (bottom panel), the signal is dominated by the NV^0 contribution, demonstrating the DUV neutralizing effect.

https://doi.org/10.1021/acs.nanolett.4c04657
Nano Lett. 2025, 25, 673−680

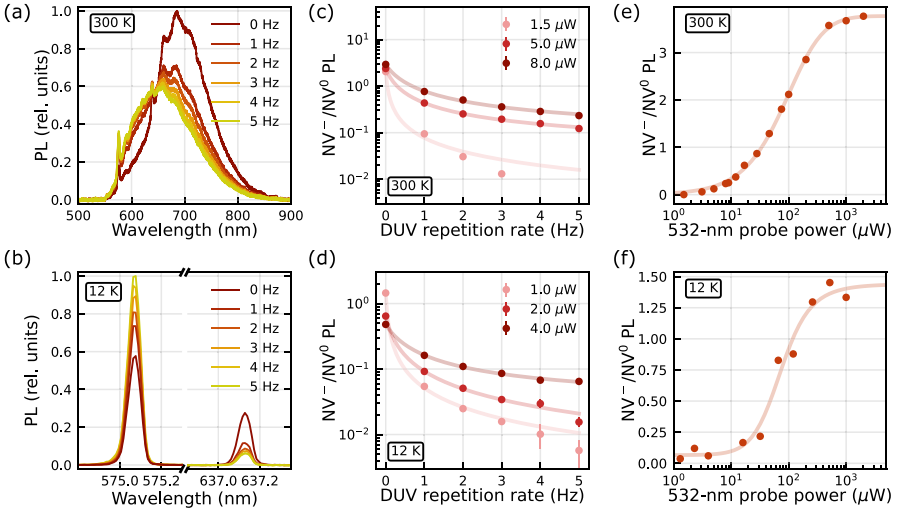

Figure 2. Neutralization of the NV center. (a, b) NV center PL under 8 μW 532 nm probe at different DUV pump repetition rates at room temperature and 12 K, respectively. A repetition rate of 0 Hz corresponds to the DUV laser being turned off. (c, d) Average PL intensity ratio of NV^-/NV^0 as a function of DUV repetition rate for different powers, also at room temperature and 12 K, respectively. (e, f) Average PL intensity ratio of NV^-/NV^0 as a function of 532 nm probe power under 5 Hz DUV pump, also at room temperature and 12 K, respectively. In (c)−(f), the solid lines represent fits to the model eq 1 with additional discussion in SI.4. For most data points the error bar is smaller than the marker.

We first examine the quasi-steady-state neutralization of bulk NV centers in sample A under simultaneous exposure to the pulsed DUV pump and a 532 nm green probe. The dominant charge states of the NV center, NV^0 and NV^-, both emit in the visible/NIR wavelength range (with zero-phonon line (ZPL) at 575 and 637 nm respectively) and can be optically excited into the phonon sideband (PSB) by 532 nm excitation making the center an ideal probe for studying neutralization.

Figures 2a,b shows the quasi-steady-state spectra of the NV center under varying DUV laser repetition rates, at both 300 and 12 K, respectively. In the absence of DUV pumping (0 Hz), the spectrum exhibits characteristic overlapping NV^0 and NV^- contributions on roughly the same order of magnitude. When the DUV is turned on at even the lowest repetition rate (1 Hz), the spectrum exhibits a dramatic decrease in the NV^- contribution, indicating a significant neutralization. Increasing the DUV repetition rate further results in an increased NV^0 contribution, limited by the probe-induced charge cycling from NV^0 to NV^-. At the 5 Hz DUV rate, the probe-only time is 2000× longer than the DUV pulse time.

To quantitatively study the effect of the DUV pulse, we performed a fitting procedure to determine the relative contributions of NV^- and NV^0. At low temperatures this is achieved by fitting of the respective ZPLs to a Voigt line shape to remove the background and then integrating. At room temperature, extracting the relative contributions of the two charge states is complicated by the overlap of the NV^0 and NV^- signals. While several techniques exist for decomposing composite spectra,[39] we instead assume that the spectrum corresponding to the lowest probe power (1.5 μW) and highest DUV repetition rate (5 Hz) constitutes a pure NV^0 signal. This assumption is consistent with the lack of a detectable NV^- ZPL at 637 nm up to a relative contribution of NV^- of less than 0.1% (SI.3). We are then able to decompose the measured spectra into the corresponding NV^- and NV^0 "basis" spectra (normalized to have equal integral, i.e., total counts). Further details are provided in SI.3. The ratio of NV^- to NV^0 PL intensities, I_{NV^-}/I_{NV^0}, under quasi-steady-state illumination of the CW 532 nm laser and pulsed DUV are shown in Figure 2c−f. The PL intensity ratio is proportional but not equal to the population ratio $\langle N_{NV^-}\rangle/\langle N_{NV^0}\rangle$ due to the difference in emission properties of both charge states. We assume $I_{NV^-}/I_{NV^0} \approx 2.5\langle N_{NV^-}\rangle/\langle N_{NV^0}\rangle$[39] which we verify in SI.3.

Figures 2c,d show the dependence on the DUV laser repetition rate for several 532 nm probe powers at 300 and 12 K, respectively. Figures 2e,f similarly show the dependence on the probe power at a constant (5 Hz) DUV repetition rate. We observe the same qualitative behavior at both temperatures; the NV signal becomes increasingly neutralized with higher DUV repetition rates and lower probe powers.

We model the population dynamics under DUV and CW probe excitation using an empirical rate equation model (SI.4). We find that the population ratio can be described by

$$\frac{\langle N_{NV^-}\rangle}{\langle N_{NV^0}\rangle} = \frac{\Gamma_-^{DUV}\delta + \gamma_-^{eff}T}{\Gamma_+^{DUV}\delta + \gamma_+^{eff}T} \tag{1}$$

where $\Gamma_\pm^{DUV}$ and $\gamma_\pm^{eff}$ are the DUV- and probe-induced charge conversion rates, whereas δ and T are the DUV pulse length and pulse period, respectively. The subscript $\pm$ indicates if the corresponding process increases ($NV^- \rightarrow NV^0$) or decreases ($NV^0 \rightarrow NV^-$) the charge of the NV center. These rates encompass not only direction ionization (e.g., $NV^- \rightarrow NV^0 + e^-$) but also charge capture (e.g., $NV^0 + e^- \rightarrow NV^-$). This model accurately describes the general dependence of the population ratio as a function of the DUV pulse rate and green power, as shown in Figures 2c−f. Details of the model and its fitting to the data are discussed in depth in SI.4.

While the model accurately describes qualitative features of the population dynamics, it is phenomenological and thus incapable of distinguishing between specific processes. Nevertheless we are able to determine the relative rates. Specifically, we find that the DUV-mediated charge neutralization (which converts $NV^- \rightarrow NV^0$) occurs at a rate of up to 5 orders of magnitude faster than either of the probe-mediated conversion processes (which are generally within 1 order of magnitude of each other; SI.4). This is despite at least a 100-fold lower DUV

https://doi.org/10.1021/acs.nanolett.4c04657
Nano Lett. 2025, 25, 673−680

excitation intensity. Additionally we find that the population dependence on the probe power (Figure 2e,f) is largely dominated by one-photon-like processes (which scale linearly with probe power), indicating that the probe-mediated charge conversion occurs primarily through the capture of charges emitted from other defects (e.g., substitutional nitrogen and/or NVH). These results indicate that the overall effect of the DUV can be straightforwardly understood despite the complexity of the NV center's charge dynamics and its interactions with other defects.

We now turn our attention to Sample B that contains bulk SiV centers. Compared to the NV center, these measurements are complicated by the inability to excite both charge states simultaneously with the same laser source[34,35] and additional participating charge states.[29,40] We thus examine SiV^- and SiV^0 separately, first considering the negatively charged SiV^-.

Figure 3a shows the quasi-steady-state PL of the SiV^- ZPL lines under a CW 532 nm probe (10 μW) and DUV pulsed laser (5 Hz) at 12 K. We observe the suppression of the SiV^- ZPL intensity by about a factor of 2, indicating bleaching of the SiV^- into an alternative charge state. While the specific charge state being generated cannot be ascertained from this measurement alone, subsequent measurements strongly suggest that the bleaching corresponds to neutralization into SiV^0.

Figure 3b shows a time trace of the SiV^- ZPL intensity as the DUV is turned on (at t = 0 s) and off (at t = 300 s). Immediately after starting the DUV, the ZPL drops in intensity, reaching a new quasi-equilibrium after about 30 s, wherein the intensity has dropped by about a factor of 2. Turning off the DUV at around t = 300 s initiates an exponential-like recovery of the ZPL which is understood to be a result of probe-induced reionization into SiV^-. Similar behavior is observed in the empirical rate equation model used to describe the NV center measurements (SI.4).

We investigate the recovery behavior of SiV^- by using time-correlated PL measurements at room temperature. The DUV laser, set to 5-Hz repetition rate, triggers the start of a detection window over which the SiV^- PL is monitored. Figure 4a shows the time-resolved PL signal for the first 100 ms after the DUV pulse (at t = 0 s). After a rapid initial decay of the SiV^- PL during the 100 μs DUV pulse, we observe an exponential-like recovery of the PL intensity with a strong dependence on the probe laser power. We find that a triple-

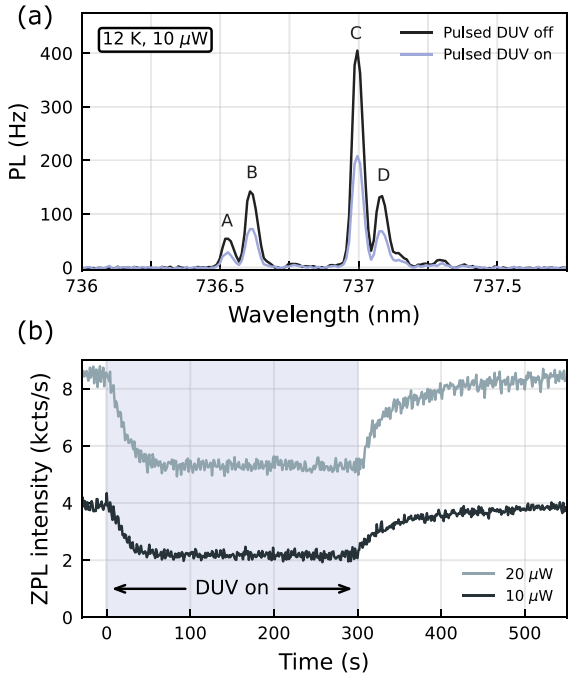

Figure 3. Bleaching of SiV^- PL. (a) Low-temperature (12 K) PL of SiV^- centers under 10 μW 532 nm probe with and without the DUV pump (1 Hz). For this power, the SiV PL is reduced by approximately a factor of 2 under DUV pumping evenly across the four primary transitions labeled A–D. (b) Integrated ZPL intensity as a function of time, initially starting with the DUV pump off (t < 0 s). The DUV pump (1 Hz) is turned on at approximately t = 0 causing a slow bleaching of the ZPL until a new equilibrium is established after about 30 s, or approximately 30 pulses. At approximately t = 300 s, the DUV pump is turned off and a slow exponential-like recovery of the SiV^- PL is observed.

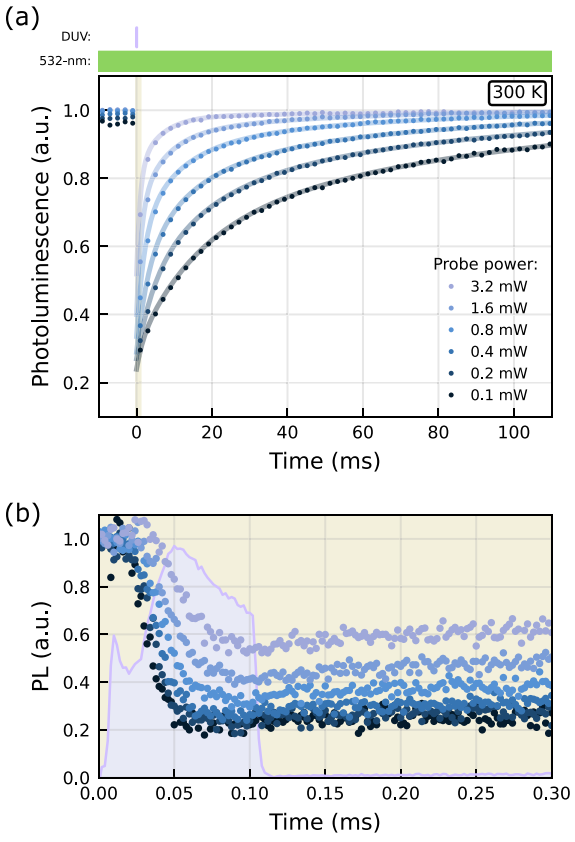

Figure 4. Time dynamics of SiV^- recharging. (a) Time-resolved photoluminescence intensity of SiV^- under DUV pulsing at 5 Hz and CW 532 nm probe excitation at various powers, along with corresponding fit to a triple-exponential (solid lines). The corresponding time constants span 2 orders of magnitude from 1–100 ms. The plotted points (circles) are sparse samples of a lower-resolution binning (2 ms resolution) to aid in readability. The fit does not include the rapid bleaching during the DUV pulse shown in (b). Additional information about the fit is included in SI.5. (b) Bleaching of the PL signal induced by the DUV pulse near time t = 0 s (indicated in (a) by the gold-colored stripe). The DUV pulse, shown in purple, lasts for 100 μs and was measured by direct excitation of NV^0 with the DUV laser. Because of the short NV^0 optical lifetime, the PL tracks the pulse intensity closely and is consistent with the laser pulse's shape as measured by a photodiode integrated within the 225 nm laser.

https://doi.org/10.1021/acs.nanolett.4c04657
Nano Lett. 2025, 25, 673–680

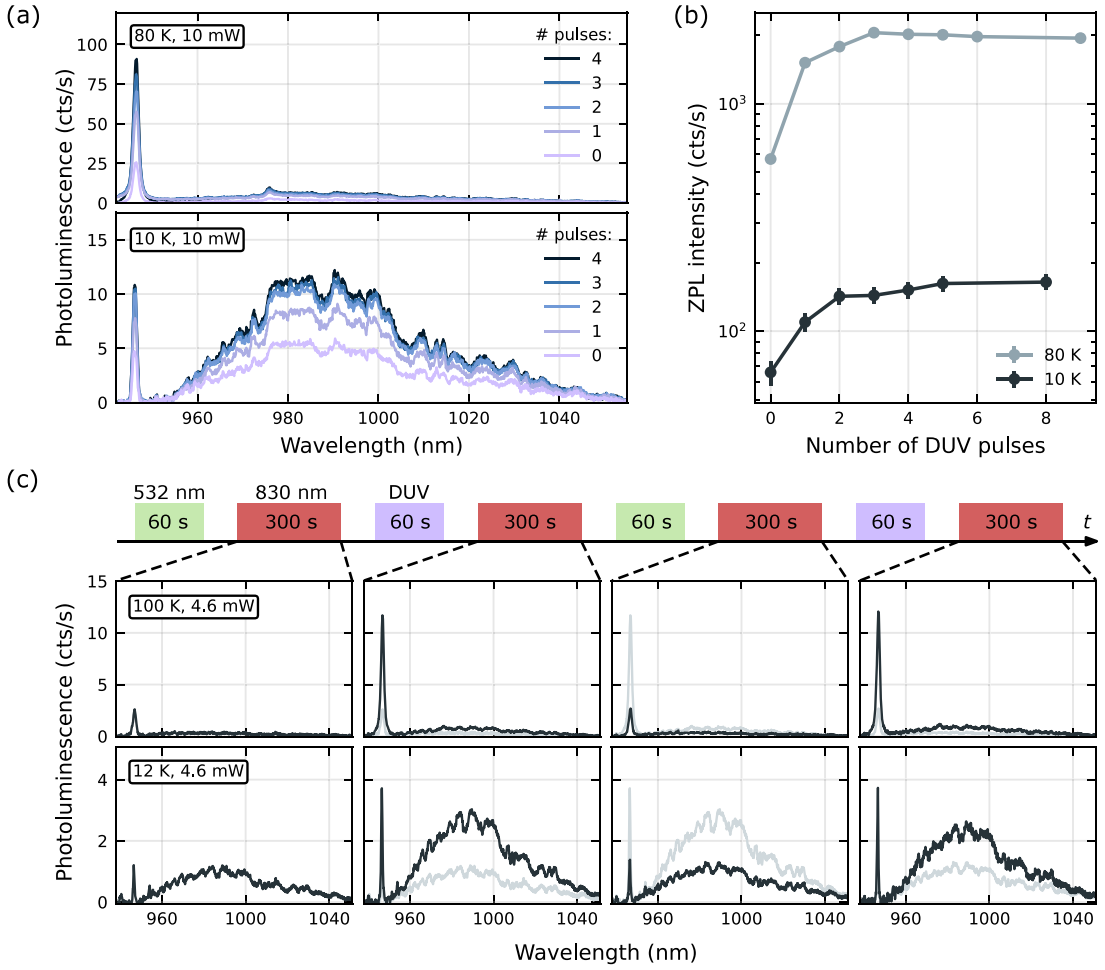

Figure 5. Neutralization of SiV. (a) A series of SiV^0 spectra taken with a 10 mW 830 nm probe laser after sequential exposure to single DUV pulses at 10 K. (b) Intensity of the ZPL line at 945 nm as a function of the number of DUV pulses. We observe similar qualitative dependence at both 10 and 80 K. The error bars correspond to shot noise. (c) Sequence of spectra after alternating exposure to 532 nm and DUV. The SiV^0 PL cycles between dark (after 532 nm exposure) to bright (after DUV exposure) repeatedly with the previous cycle's spectrum shown in gray.

exponential curve accurately describes the PL recovery, while also minimizing the number of parameters. The fitted time constants span the full measurable range of 1−100 ms which suggests that the recovery is complex, likely including multiple processes. We do not attempt to identify specific processes here, but note that similar nonexponential time evolution has been observed in intraband-gap photodoping.[30]

Figure 4b shows the same time-resolved PL in higher resolution during and immediately after the DUV pulse. We observe up to 80% reduction in the SiV^- PL over the duration of the 100 μs pulse (shown in purple). This suggests that the DUV can rapidly modify the defect charge states; the comparatively long DUV exposure times used in prior work is not required.[32−34]

We perform PL measurements of SiV^0 to confirm that SiV^- is neutralized by the DUV. We monitor the SiV^0 population via PL excited by an 830 nm CW diode laser. The 830 nm excitation is unable to directly ionize SiV^0 as it falls below the 1.5 eV photoionization threshold;[34,35] nor is it able to ionize carriers from other defects such as vacancies, nitrogen-vacancies, or substitutional nitrogen.[38] This enables the use of prolonged 830 nm excitation, even at high powers exceeding 1 mW (SI.6).

We utilized the CW 532 nm laser as a pump to initialize the SiV into SiV^- by exposing the sample at 1 mW for 60 s before reading out the SiV^0 population with the 830 nm laser (10 mW). We next drive the sample with a single DUV pulse before measuring out the population again, repeating this process until the signal asymptotes to its maximal value. The corresponding spectra are plotted in Figure 5a showing a significant enhancement of the SiV^0 ZPL peak by over a factor of 2 after only two DUV pulses. Figure 5b shows the ZPL intensities as a function of the number of DUV pulses at both 10 and 80 K which have very similar trends. The rapid saturation of the ZPL intensity after the first few pulses is consistent with the rapid bleaching of the SiV^- signal shown in Figure 4. Details of the SiV^0 spectral analysis are discussed in SI.6.

The SiV^0 spectra are markedly different at 10 and 80 K. Specifically, the 946 nm ZPL is greatly enhanced and the PSB seemingly diminished at elevated temperatures. Such behavior is explained by the presence of two excited states, ^3E_u and $^3A_{2u}$, corresponding to the 946 and 951 nm ZPL, respectively, that have been directly observed in uniaxial stress measurements.[41] Due to the 6.8 meV splitting, the ^3E_u state becomes frozen out at low temperatures, and thus, its 946 nm ZPL and relatively small PSB drop in intensity. The large PSB seen at 10 K comes

https://doi.org/10.1021/acs.nanolett.4c04657
Nano Lett. 2025, 25, 673−680

instead from the 951 nm ZPL emission from the $^3A_{2u}$ state, which has a higher population at this temperature.

We next examine the repeatability of the photoinduced charge cycling. Figure 5c shows the SiV^0 spectra after repeated cycling between 300 s PL measurements with the 830 nm probe (4.6 mW) and 60 s pump steps using either 532 nm or DUV pumps to ionize or neutralize the SiV respectively. We observe nearly identical spectra after a full cycle, indicating that the population can be reliably initialized into SiV^0 by the DUV excitation. Such repeatable initialization, in combination with the stability of SiV^0 under 830 nm excitation (SI.6), demonstrates the viability of DUV exposure as a fundamental tool for SiV^0-based quantum technologies.

We have demonstrated fast and on-demand neutralization of NV and SiV centers in diamond via above-band gap, DUV excitation. Using DUV to reliably neutralize the defects, we investigated the charge-state dynamics of the NV and SiV centers under combinations of CW probe excitation and DUV pumping. These results and their agreement with our modeling indicate that the effect of the DUV is well understood and useful for defect-based applications. The technique also directly generates the neutral SiV^0 without high-concentration codoping which may accelerate the development of SiV^0-based quantum nodes.

Beyond NV or SiV, this technique is agnostic to the structure and type of defect and may be applied to study the neutral charge states of other interesting color centers, such as the group-IV germanium-, tin-, and lead-vacancy centers. This effect is also not limited to optically active defects but might also be used to neutralize nearby undesired defects present in the host lattice, which could contribute to electric-field noise. This can even be applied to neutralize the environment of charged color centers provided low-energy intragap excitation to reinitialize the target center minimally perturbs the neutralized environment. The neutralized environment would have reduced electric-field noise which has been associated with spectral diffusion and inhomogeneous broadening.[42] Finally, we remark that this technique will be applicable in other emerging quantum defect host lattices.[3,4]

■ ASSOCIATED CONTENT

Supporting Information

The Supporting Information is available free of charge at https://pubs.acs.org/doi/10.1021/acs.nanolett.4c04657.

Schematic of experimental setup, estimation of DUV-induced photoionization rates and carrier densities, description of ab initio calculations, process and details of decomposition of room-temperature NV center photoluminescence, theoretical rate model description with application to data, measurement and analysis description for time-resolved SiV^- center data, and analysis and stability of SiV^0 center data (PDF)

■ AUTHOR INFORMATION

Corresponding Authors

Christian Pederson − *University of Washington, Physics Department, Seattle, Washington 98105, United States*; Email: cpederso@uw.edu

Nicholas S. Yama − *University of Washington, Electrical and Computer Engineering Department, Seattle, Washington 98105, United States*; orcid.org/0000-0002-6123-3313; Email: nsyama@uw.edu

Authors

Lane Beale − *University of Washington, Physics Department, Seattle, Washington 98105, United States*

Matthew Markham − *Element Six, Global Innovation Centre, Didcot, Oxfordshire OX11 0QR, U.K.*

Mark E. Turiansky − *US Naval Research Laboratory, Washington, D.C. 20375, United States*; orcid.org/0000-0002-9154-3582

Kai-Mei C. Fu − *University of Washington, Electrical and Computer Engineering Department, Seattle, Washington 98105, United States; University of Washington, Physics Department, Seattle, Washington 98105, United States; Physical Sciences Division, Pacific Northwest National Laboratory, Washington 99352, United States*

Complete contact information is available at: https://pubs.acs.org/10.1021/acs.nanolett.4c04657

Author Contributions

#(C.P. and N.S.Y.) These two authors contributed equally

Notes

The authors declare no competing financial interest.

■ ACKNOWLEDGMENTS

The SiV work was primarily supported by Department of Energy, Office of Science, National Quantum Information Science Research Centers, Co-design Center for Quantum Advantage (C2QA), under Contract Number DE-SC0012704. The NV work was primarily supported by the National Science Foundation through the University of Washington Materials Research Science and Engineering Center, DMR-2308979. N.S.Y. was supported by the National Science Foundation Graduate Research Fellowship Program under Grant No. DGE-2140004. M.E.T. was supported by the Office of Naval Research through the Naval Research Laboratory's Basic Research Program. We thank Nathalie de Leon, Carlos Meriles, and Chris Van de Walle for helpful discussions.

■ REFERENCES

(1) Aharonovich, I.; Englund, D.; Toth, M. Solid-state single-photon emitters. *Nat. Photonics* **2016**, *10* (10), 631−641.

(2) Atatüre, M.; Englund, D.; Vamivakas, N.; Lee, S.-Y.; Wrachtrup, J. Material platforms for spin-based photonic quantum technologies. *Nature Reviews Materials* **2018**, *3* (5), 38−51.

(3) Bassett, L. C.; Alkauskas, A.; Exarhos, A. L.; Fu, K.-M. C. Quantum defects by design. *Nanophotonics* **2019**, *8* (11), 1867−1888.

(4) Wolfowicz, G.; Heremans, F. J.; Anderson, C. P.; Kanai, S.; Seo, H.; Gali, A.; Galli, G.; Awschalom, D. D. Quantum guidelines for solid-state spin defects. *Nature Reviews Materials* **2021**, *6* (10), 906−925.

(5) Schirhagl, R.; Chang, K.; Loretz, M.; Degen, C. L. Nitrogen-vacancy centers in diamond: Nanoscale sensors for physics and biology. *Annu. Rev. Phys. Chem.* **2014**, *65*, 83−105.

(6) Knaut, C. M.; Suleymanzade, A.; Wei, Y. C.; Assumpcao, D. R.; Stas, P. J.; Huan, Y. Q.; Machielse, B.; Knall, E. N.; Sutula, M.; Baranes, G.; Sinclair, N.; De-Eknamkul, C.; Levonian, D. S.; Bhaskar, M. K.; Park, H.; Lončar, M.; Lukin, M. D. Entanglement of nanophotonic quantum memory nodes in a telecom network. *Nature* **2024**, *629* (8012), 573−578.

(7) Rose, B. C.; Huang, D.; Zhang, Z.-H.; Stevenson, P.; Tyryshkin, A. M.; Sangtawesin, S.; Srinivasan, S.; Loudin, L.; Markham, M. L.; Edmonds, A. M.; Twitchen, D. J.; Lyon, S. A.; de Leon, N. P. Observation of an environmentally insensitive solid-state spin defect in diamond. *Science* **2018**, *361* (6397), 60−63.

(8) Radishev, D.; Lobaev, M.; Bogdanov, S.; Gorbachev, A.; Vikharev, A.; Drozdov, M. Investigation of nv centers charge states

in cvd diamond layers doped by nitrogen and phosphorous. *J. Lumin.* **2021**, *239*, 118404.
(9) Doi, Y.; Fukui, T.; Kato, H.; Makino, T.; Yamasaki, S.; Tashima, T.; Morishita, H.; Miwa, S.; Jelezko, F.; Suzuki, Y.; Mizuochi, N. Pure negatively charged state of the nv center in *n*-type diamond. *Phys. Rev. B* **2016**, *93*, 081203.
(10) Groot-Berning, K.; Raatz, N.; Dobrinets, I.; Lesik, M.; Spinicelli, P.; Tallaire, A.; Achard, J.; Jacques, V.; Roch, J.-F.; Zaitsev, A. M.; Meijer, J.; Pezzagna, S. Passive charge state control of nitrogen-vacancy centres in diamond using phosphorous and boron doping. *physica status solidi (a)* **2014**, *211* (10), 2268−2273.
(11) Hauf, M. V.; Grotz, B.; Naydenov, B.; Dankerl, M.; Pezzagna, S.; Meijer, J.; Jelezko, F.; Wrachtrup, J.; Stutzmann, M.; Reinhard, F.; Garrido, J. A. Chemical control of the charge state of nitrogen-vacancy centers in diamond. *Phys. Rev. B* **2011**, *83*, 081304.
(12) Fu, K.-M. C.; Santori, C.; Barclay, P. E.; Beausoleil, R. G. Conversion of neutral nitrogen-vacancy centers to negatively charged nitrogen-vacancy centers through selective oxidation. *Appl. Phys. Lett.* **2010**, *96*, 121907.
(13) Stacey, A.; Dontschuk, N.; Chou, J.-P.; Broadway, D. A.; Schenk, A. K.; Sear, M. J.; Tetienne, J.-P.; Hoffman, A.; Prawer, S.; Pakes, C. I.; Tadich, A.; de Leon, N. P.; Gali, A.; Hollenberg, L. C. L. Evidence for primal sp2 defects at the diamond surface: Candidates for electron trapping and noise sources. *Advanced Materials Interfaces* **2019**, *6* (3), 1801449.
(14) Pederson, C.; Giridharagopal, R.; Zhao, F.; Dunham, S. T.; Raitses, Y.; Ginger, D. S.; Fu, K.-M. C. Optical tuning of the diamond fermi level measured by correlated scanning probe microscopy and quantum defect spectroscopy. *Phys. Rev. Mater.* **2024**, *8*, 036201.
(15) Zhang, Z.-H.; Edmonds, A. M.; Palmer, N.; Markham, M. L.; de Leon, N. P. Neutral silicon-vacancy centers in diamond via photoactivated itinerant carriers. *Phys. Rev. Appl.* **2023**, *19*, 034022.
(16) Rodgers, L. V. H.; Nguyen, S. T.; Cox, J. H.; Zervas, K.; Yuan, Z.; Sangtawesin, S.; Stacey, A.; Jaye, C.; Weiland, C.; Pershin, A.; Gali, A.; Thomsen, L.; Meynell, S. A.; Hughes, L. B.; Jayich, A. C. B.; Gui, X.; Cava, R. J.; Knowles, R. R.; de Leon, N. P. Diamond surface functionalization via visible light−driven c−h activation for nanoscale quantum sensing. *Proc. Natl. Acad. Sci. U. S. A.* **2024**, *121* (11), No. e2316032121.
(17) Walukiewicz, W. Amphoteric native defects in semiconductors. *Appl. Phys. Lett.* **1989**, *54*, 2094−2096.
(18) Schreyvogel, C.; Polyakov, V.; Wunderlich, R.; Meijer, J.; Nebel, C. E. Active charge state control of single NV centres in diamond by in-plane Al-Schottky junctions. *Sci. Rep.* **2015**, *5*, 12160.
(19) Widmann, M.; Niethammer, M.; Fedyanin, D. Y.; Khramtsov, I. A.; Rendler, T.; Booker, I. D.; Ul Hassan, J.; Morioka, N.; Chen, Y.-C.; Ivanov, I. G.; Son, N. T.; Ohshima, T.; Bockstedte, M.; Gali, A.; Bonato, C.; Lee, S.-Y.; Wrachtrup, J. Electrical charge state manipulation of single silicon vacancies in a silicon carbide quantum optoelectronic device. *Nano Lett.* **2019**, *19*, 7173−7180.
(20) Kato, H.; Wolfer, M.; Schreyvogel, C.; Kunzer, M.; Müller-Sebert, W.; Obloh, H.; Yamasaki, S.; Nebel, C. Tunable light emission from nitrogen-vacancy centers in single crystal diamond PIN diodes. *Appl. Phys. Lett.* **2013**, *102*, 151101.
(21) Rieger, M.; Villafañe, V.; Todenhagen, L. M.; Matthies, S.; Appel, S.; Brandt, M. S.; Müller, K.; Finley, J. J. Fast optoelectronic charge state conversion of silicon vacancies in diamond. *Science Advances* **2024**, *10* (8), No. eadl4265.
(22) Dhomkar, S.; Henshaw, J.; Jayakumar, H.; Meriles, C. A. Long-term data storage in diamond. *Science Advances* **2016**, *2* (10), No. e1600911.
(23) Monge, R.; Delord, T.; Meriles, C. A. Reversible optical data storage below the diffraction limit. *Nat. Nanotechnol.* **2024**, *19*, 202−207.
(24) Li, C. X.; Zhang, Q. Y.; Zhou, N.; Hu, B. C.; Ma, C. Y.; Zhang, C.; Yi, Z. UV-induced charge-state conversion from the negatively to neutrally charged nitrogen-vacancy centers in diamond. *J. Appl. Phys.* **2022**, *132*, 215102.
(25) Völker, L. A.; Herb, K.; Merchant, D. A.; Bechelli, L.; Degen, C. L.; Abendroth, J. M. Charge and spin dynamics and destabilization of shallow nitrogen−vacancy centers under uv and blue excitation. *Nano Lett.* **2024**, *24*, 11895−11903.
(26) Zuber, J. A.; Li, M.; Grimau Puigibert, M. l.; Happacher, J.; Reiser, P.; Shields, B. J.; Maletinsky, P. Shallow silicon vacancy centers with lifetime-limited optical linewidths in diamond nanostructures. *Nano Lett.* **2023**, *23* (12), 10901−10907.
(27) Lozovoi, A.; Jayakumar, H.; Daw, D.; Vizkelethy, G.; Bielejec, E.; Doherty, M. W.; Flick, J.; Meriles, C. A. Optical activation and detection of charge transport between individual colour centres in diamond. *Nature Electronics* **2021**, *4*, 717−724.
(28) Lozovoi, A.; Vizkelethy, G.; Bielejec, E.; Meriles, C. A. Imaging dark charge emitters in diamond via carrier-to-photon conversion. *Science Advances* **2022**, *8* (1), No. eabl9402.
(29) Wood, A.; Lozovoi, A.; Zhang, Z.-H.; Sharma, S.; López-Morales, G. I.; Jayakumar, H.; de Leon, N. P.; Meriles, C. A. Room-temperature photochromism of silicon vacancy centers in CVD diamond. *Nano Lett.* **2023**, *23* (3), 1017−1022.
(30) Garcia-Arellano, G.; López-Morales, G. I.; Manson, N. B.; Flick, J.; Wood, A. A.; Meriles, C. A. Photo-induced charge state dynamics of the neutral and negatively charged silicon vacancy centers in room-temperature diamond. *Advanced Science* **2024**, *11* (22), 2308814.
(31) Naka, N.; Morimoto, H.; Akimoto, I. Excitons and fundamental transport properties of diamond under photo-injection. *physica status solidi (a)* **2016**, *213* (10), 2551−2563.
(32) Khan, R. U. A.; Martineau, P. M.; Cann, B. L.; Newton, M. E.; Twitchen, D. J. Charge transfer effects, thermo and photochromism in single crystal cvd synthetic diamond. *J. Phys.: Condens. Matter* **2009**, *21*, 364214.
(33) Khan, R. U. A.; Cann, B. L.; Martineau, P. M.; Samartseva, J.; Freeth, J. J. P.; Sibley, S. J.; Hartland, C. B.; Newton, M. E.; Dhillon, H. K.; Twitchen, D. J. Colour-causing defects and their related optoelectronic transitions in single crystal cvd diamond. *J. Phys.: Condens. Matter* **2013**, *25*, 275801.
(34) D'Haenens-Johansson, U. F. S.; Edmonds, A. M.; Green, B. L.; Newton, M. E.; Davies, G.; Martineau, P. M.; Khan, R. U. A.; Twitchen, D. J. Optical properties of the neutral silicon split-vacancy center in diamond. *Phys. Rev. B* **2011**, *84*, 245208.
(35) Zhang, Z.-H.; Stevenson, P.; Thiering, G. m. H.; Rose, B. C.; Huang, D.; Edmonds, A. M.; Markham, M. L.; Lyon, S. A.; Gali, A.; de Leon, N. P. Optically detected magnetic resonance in neutral silicon vacancy centers in diamond via bound exciton states. *Phys. Rev. Lett.* **2020**, *125*, 237402.
(36) Takiyama, K.; Abd-Elrahman, M.; Fujita, T.; Oda, T. Photoluminescence and decay kinetics of indirect free excitons in diamonds under the near-resonant laser excitation. *Solid State Commun.* **1996**, *99* (11), 793−797.
(37) Saeedi, K.; Simmons, S.; Salvail, J. Z.; Dluhy, P.; Riemann, H.; Abrosimov, N. V.; Becker, P.; Pohl, H.-J.; Morton, J. J. L.; Thewalt, M. L. W. Room-temperature quantum bit storage exceeding 39 minutes using ionized donors in silicon-28. *Science* **2013**, *342* (6160), 830−833.
(38) Bourgeois, E.; Londero, E.; Buczak, K.; Hruby, J.; Gulka, M.; Balasubramaniam, Y.; Wachter, G.; Stursa, J.; Dobes, K.; Aumayr, F.; Trupke, M.; Gali, A.; Nesladek, M. Enhanced photoelectric detection of nv magnetic resonances in diamond under dual-beam excitation. *Phys. Rev. B* **2017**, *95*, 041402.
(39) Alsid, S. T.; Barry, J. F.; Pham, L. M.; Schloss, J. M.; O'Keeffe, M. F.; Cappellaro, P.; Braje, D. A. Photoluminescence decomposition analysis: A technique to characterize N-*v* creation in diamond. *Phys. Rev. Appl.* **2019**, *12*, 044003.
(40) Breeze, B. G.; Meara, C. J.; Wu, X. X.; Michaels, C. P.; Gupta, R.; Diggle, P. L.; Dale, M. W.; Cann, B. L.; Ardon, T.; D'Haenens-Johansson, U. F. S.; Friel, I.; Rayson, M. J.; Briddon, P. R.; Goss, J. P.; Newton, M. E.; Green, B. L. Doubly charged silicon vacancy center, si-n complexes, and photochromism in n and si codoped diamond. *Phys. Rev. B* **2020**, *101*, 184115.

https://doi.org/10.1021/acs.nanolett.4c04657
Nano Lett. 2025, 25, 673−680

(41) Green, B. L.; Doherty, M. W.; Nako, E.; Manson, N. B.; D'Haenens-Johansson, U. F. S.; Williams, S. D.; Twitchen, D. J.; Newton, M. E. Electronic structure of the neutral silicon-vacancy center in diamond. *Phys. Rev. B* **2019**, *99*, 161112.
(42) Tamarat, P.; Gaebel, T.; Rabeau, J. R.; Khan, M.; Greentree, A. D.; Wilson, H.; Hollenberg, L. C. L.; Prawer, S.; Hemmer, P.; Jelezko, F.; Wrachtrup, J. Stark shift control of single optical centers in diamond. *Phys. Rev. Lett.* **2006**, *97*, 083002.

https://doi.org/10.1021/acs.nanolett.4c04657
Nano Lett. 2025, 25, 673−680